

Organic & Biomolecular Chemistry

www.rsc.org/obc

Volume 11 | Number 34 | 14 September 2013 | Pages 5549–5736



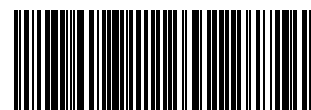
ISSN 1477-0520

RSC Publishing

PAPER

Byeang Hyeon Kim *et al.*

DNSC: a fluorescent, environmentally sensitive cytidine derivative for the direct detection of GGG triad sequences



1477-9226 (2013) 42:34;1-J

^{DN5}C: a fluorescent, environmentally sensitive cytidine derivative for the direct detection of GGG triad sequences†

Cite this: *Org. Biomol. Chem.*, 2013, **11**, 5605

Ki Tae Kim,^a Hyun Woo Kim,^b Dohyun Moon,^c Young Min Rhee^b and Byeang Hyeon Kim^{*a}

With the goal of developing a fluorescent nucleoside sensitive to its environment, in this study we synthesized ^{DN5}C, a novel modified 2'-deoxycytidine bearing a 5-(dimethylamino)naphthalene-1-sulfonyl (dansyl) moiety at the N4 position, and tested its properties in monomeric and oligomeric states. ^{DN5}C undergoes intramolecular photoinduced electron transfer between its dansyl and cytosine units, resulting in remarkable changes in fluorescence that depend on the choice of solvent. In addition, the fluorescence behavior and thermal stability of oligonucleotides containing ^{DN5}C are dependent on the nature of the flanking and neighboring bases. Notably, ^{DN5}C exhibits fluorescence enhancement only in fully matched duplex DNA containing a GGG triad sequence. The environmental sensitivity of ^{DN5}C can be exploited as a fluorescence tool for monitoring the interactions of DNA with other biomolecules, including DNA, RNA, and proteins.

Received 13th June 2013,
Accepted 25th June 2013

DOI: 10.1039/c3ob41222a

www.rsc.org/obc

Introduction

The development of new fluorescent probes to investigate specific DNA sequences or the interactions of DNA with other biomolecules remains a considerable challenge. Many fluorescent nucleic acid probes have been designed over the years to detect specific sequences and single nucleotide polymorphisms (SNPs),^{1–3} to monitor the binding of targets to DNA,⁴ to detect specific enzymes,^{5,6} and to investigate nucleic acid structures and functions.^{7,8} Commonly, fluorescent nucleosides have been synthesized and incorporated into nucleic acid probes to impart them with unique properties, such as site-specific responses (e.g., toward SNPs), micro-environmental sensitivity, or high brightness.^{9–11} Nevertheless, the

application of these fluorescent nucleic acids remains limited because of various drawbacks, which are expected to be overcome through better design of novel types of fluorescent nucleosides.¹¹

One of the general limitations of fluorescent DNA probes is their susceptibility to quenching phenomena induced by neighboring bases. In particular, fluorophores are commonly quenched through photoinduced electron transfer (PET) to guanine bases in DNA strands.¹² Accordingly, previous fluorescence probes developed in our group, and in others, have exhibited very low fluorescence intensity and sensitivity when their target DNA strands have featured a series of guanine (G)-rich sequences.¹³ Unfortunately, series of G bases appear frequently in many biologically important DNA sequences, including telomeric DNA strands,¹⁴ oncogene promoter regions,¹⁵ codons for glycine, and CpG island regions.¹⁶ Moreover, mutations in consecutive G sequences have been an important issue since the G-tract acts as a core sequence of the binding site for transcription factors¹⁷ or is closely related to HIV-1 reverse transcription.¹⁸ Therefore, the development of novel fluorescent nucleic acids that exhibit higher fluorescence in the presence of a G-rich sequence than in the presence of other sequences will be necessary if we are to improve the general applicability of fluorescent probes. Notably, to the best of our knowledge there are no previously reported examples of the direct sensing of the GGG triple sequence.

The 5-(dimethylamino)naphthalene-1-sulfonyl (dansyl) group is a practical fluorophore used widely in protein sequencing

^aDepartment of Chemistry, BK School of Molecular Science, Pohang University of Science and Technology (POSTECH), Pohang 790-784, South Korea.

E-mail: bhkim@postech.ac.kr; Fax: +82 54-279-3399; Tel: +82 54-279-5856

^bDepartment of Chemistry, Center for Self-assembly and Complexity, Institute for Basic Science, Pohang University of Science and Technology (POSTECH), Pohang 790-784, South Korea. E-mail: ymrhee@postech.ac.kr

^cBeamline Division, Pohang Accelerator Laboratory, Pohang University of Science and Technology (POSTECH), Pohang 790-784, South Korea.

E-mail: dmoon@postech.ac.kr; Tel: +82 54-279-1547

†Electronic supplementary information (ESI) available: Supporting figures and graphs, additional UV absorption and fluorescence emission spectra, NMR titration results, crystallographic data and MALDI-TOF MS analysis of ODNs. CCDC 930728. For ESI and crystallographic data in CIF or other electronic format see DOI: 10.1039/c3ob41222a

and amino acid analysis. In addition, the dansyl fluorophore has also been used as the reporting part of fluorescent DNA systems because of its large Stokes shifts, intense absorption bands, strong fluorescence, and high sensitivity to the hydrophobicity of its environment.¹⁹ In previous examples of chemical conjugation to nucleosides, dansyl groups have been attached to the 2'-OH, C-5, and C-8 positions of the nucleosides^{20–22} to obtain probes for monitoring the interactions between DNA strands, between DNA and ligands, or to rationally design multiple fluorescent DNA probes. Notably, the fluorescence of the dansyl group is very sensitive to its position in the nucleoside or DNA strand and to the polarity of its environment. For example, oligonucleotides with dansyl linked by a relatively short linker at C-5 position of pyrimidine exhibited little or no change in fluorescence by duplex formation while the dansyl group at the C-8 position of purine exhibited an enhancement of fluorescence intensity.²⁰ Based on these previous reports, we expected that direct conjugation of a dansyl group in the region of a nucleobase that undergoes hydrogen bonding might lead to greater fluorescence sensitivity toward changes in single nucleotides or structural changes of DNA (*e.g.*, duplex formation). Furthermore, proximity of the base and the dansyl group may induce unique electronic interaction in the excited state.

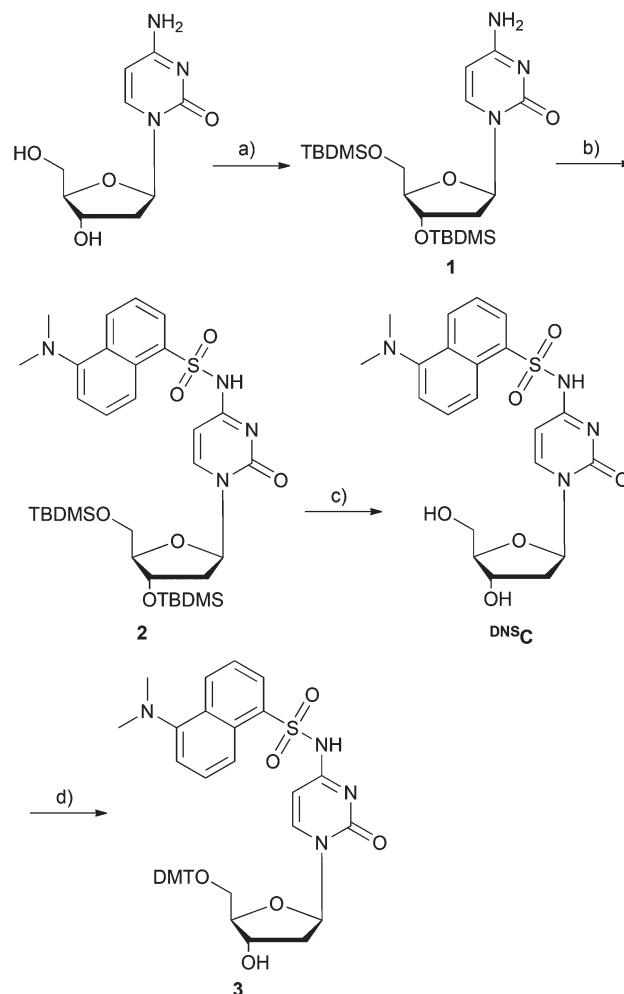
In this study, we easily synthesized the nucleoside ^{DNS}C, which features a dansyl group attached directly at the N4 position – a hydrogen bonding unit and a major groove site – of cytosine and then we monitored its fluorescence properties as well as those of oligonucleotides incorporating it. We found that ^{DNS}C exhibits unique properties for a dansyl-derivative, allowing its use as a fluorescence-on system for the GGG triplet sequence.

Results and discussion

Synthesis and photophysical properties of ^{DNS}C

To directly conjugate a dansyl group to a nucleoside through its amino group, we chose 2'-deoxycytidine as the starting material. Protecting the 3'- and 5'-OH groups of 2'-deoxycytidine through reactions with *tert*-butyldimethylsilyl chloride (TBDMS-Cl), followed by reaction with dansyl chloride and tetrabutylammonium fluoride-mediated deprotection of the TBDMS groups, we obtained compound ^{DNS}C. To incorporate ^{DNS}C into oligonucleotides, we protected ^{DNS}C through reaction with dimethoxytrityl chloride (DMT-Cl) to obtain **3**, the precursor of DNA phosphoramidite. Scheme 1 summarizes the synthetic process.

We confirmed the identities of these compounds using ¹H and ¹³C NMR spectroscopy, mass spectrometry, and melting point measurements. In addition, we obtained single crystals of ^{DNS}C through slow evaporation of MeCN from a 20 mM solution in a sealed tube. Fig. 1a displays the structure of ^{DNS}C as determined using X-ray crystallography (CCDC registry number: 930728). The individual units of ^{DNS}C featured a *syn* configuration (oxygen on C-2 is projecting toward the furanose



Scheme 1 Synthesis of ^{DNS}C and **3**. Reagents and conditions: (a) *tert*-butyldimethylsilyl chloride, imidazole, DMF, r.t., 12 h, 88%; (b) dansyl chloride, DIPEA, CH₂Cl₂, 50 °C, 24 h, 70%; (c) tetrabutylammonium fluoride, THF, r.t., 6 h, 97%; (d) 4,4'-dimethoxytrityl chloride (DMT-Cl), DIPEA, DMF, 55 °C, 24 h, 80%. TBDMS, *tert*-butyldimethylsilyl; DIPEA, *N,N*-diisopropylethylamine; DMF, *N,N*-dimethylformamide; THF, tetrahydrofuran.

ring). The planes of the cytosine and dansyl groups were aligned almost orthogonally because of the sulfonyl group. In the packing structure, we observe anti-parallel π - π interactions between the dansyl groups of pairs of ^{DNS}C units (Fig. 1b); in addition, one ^{DNS}C unit recognized another through O(5)–H(5)⋯O(6) hydrogen bonding.

Encouraged by its solid state structure, we used quantum chemical calculations to study the photophysical behavior of ^{DNS}C, analyzing three of its excited states with a developmental version of the Q-Chem software package²³ (see Table 1 and Fig. S3 in ESI[†]). We optimized the geometries at the B3LYP/6-31G(d) computational level²⁴ and determined the properties of the excited states using the SOS-CIS(D₀)/6-31G(d) method.²⁵ To incorporate an approximate solvent effect, we employed the conductor-like screening model (COSMO) by treating the solvent as a continuum having a dielectric constant ϵ of 80.²⁶ In Table 1, all computed energies are listed with respect to the

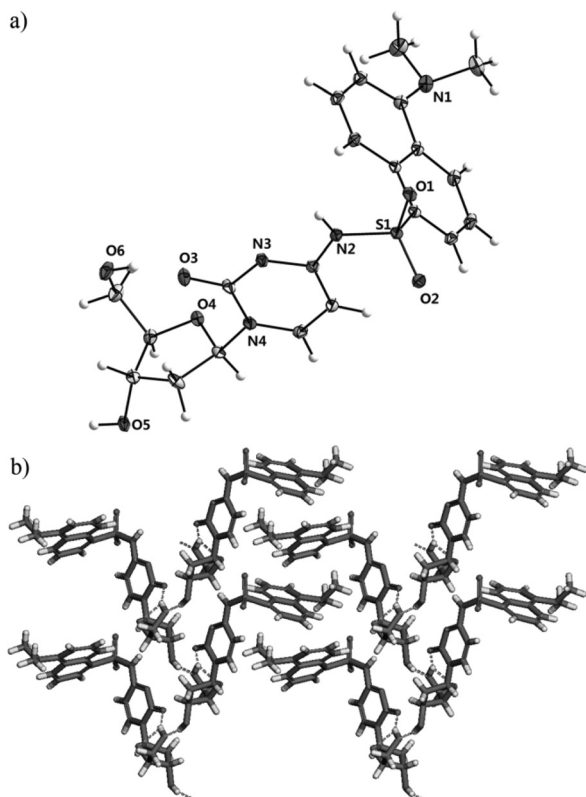


Fig. 1 (a) Solid state structure of DNS^{C} (30% probability ellipsoids) and (b) its packing in the crystal.

Table 1 Calculated excited state energies and transition characters of DNS^{C}

State ^a	Energy (kcal mol ⁻¹)		Transition character
	Vacuum	$\epsilon = 80$	
S1	98.94	96.71	Local transition at the dansyl moiety
S2	100.98	101.02	Local transition at the dansyl moiety
S3	107.5	108.72	Local transition at the base

^aThree lowest-energy singlet excited states (S1, S2, S3); see the Experimental section for computational details.

ground state energies under vacuum and in a continuum solvent. By investigating the character of each excited state, we found that the dansyl moiety was excited mainly in the S1 and S2 states, while an electronic transition at cytosine contributed significantly to the S3 state. Importantly, the energy differences among S1, S2, and S3 (4.3–12.0 kcal mol⁻¹) in the polar solvent were sufficiently small to allow internal conversions between these excited states under ambient conditions. Because excited DNA bases can dissipate energy non-radiatively,²⁷ these results implied that the fluorescence of DNS^{C} would likely be quenched through internal conversions to the state with the local electronic transition at the cytosine unit. Next, we checked the photophysical properties of DNS^{C} as solutions in CH_2Cl_2 , THF, MeOH, MeCN, DMF, DMSO, and water (Table 2). Typically, cytosine exhibits UV absorbance at

Table 2 Photophysical properties of DNS^{C}

	λ_{abs}^a (nm)	λ_{emi}^a (nm)	$\epsilon^{a,c}$ (cm ⁻¹ M ⁻¹)	$\Phi_f^{a,b}$
MeOH	295	490	48 200	0.0090
MeCN	298	474	44 700	0.010
DMF	290	470	31 000	0.54
DMSO	290	480	29 600	0.74
Water	295	520	33 700	0.0028

^a Measured at 3.3 μM at 298 K. ^b Fluorescence quantum yield measured relative to fluorescein ($\Phi_f = 0.79$) in 0.1 M NaOH. ^c Extinction coefficient.

270 nm; in contrast, DNS^{C} exhibits its value of λ_{ex} near 295 nm in aqueous solution. This bathochromic shift presumably resulted from electron withdrawal by the sulfonyl group at the N4 position. We also confirmed that the UV absorption of the original dansyl moiety was maintained for the solution of DNS^{C} in water (see Fig. S1a in ESI[†]). In the normalized UV absorption spectra of DNS^{C} , we observed an absorption band at 290–298 nm for all solvents, with a shoulder at 330 nm only for the solutions in the polar aprotic solvents DMF and DMSO (Fig. 2a). Interestingly, the fluorescence of DNS^{C} exhibited a

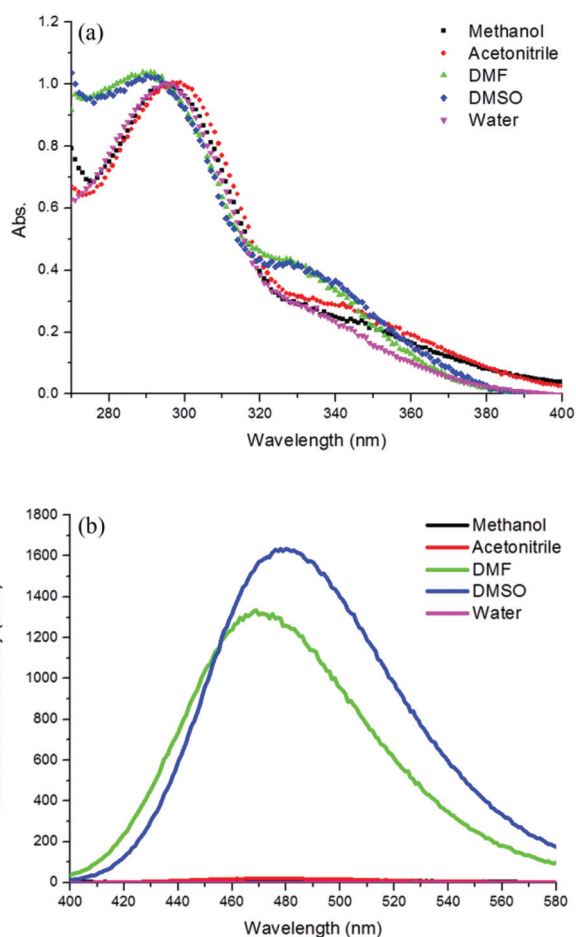


Fig. 2 (a) UV absorption and (b) fluorescence emission spectra of DNS^{C} in various solvents (concentration, 3.3 μM ; total volume, 1 mL; excitation, 295 nm, excitation and emission slit: 5 nm).

significant solvent-dependency. Firstly, we confirmed solvent-dependency of fluorescence emission by using $E_T(30)$ values (Fig. S1b in ESI†). In MeOH, MeCN, and water, ^{DNS}C displayed very low fluorescence quantum yields, whereas it provided very strong fluorescence in DMF and DMSO; for example, the fluorescence quantum yield of ^{DNS}C in DMSO was 264-fold greater than that in water (Table 2, Fig. 2b). Typically, dansylamide derivatives lacking a quencher have moderate quantum yields (*ca.* 0.26–0.53) in other solvents.²⁸ Accordingly, the very low quantum yield of ^{DNS}C in MeCN presumably arose as a result of quenching by the nucleobase. Moreover, dansylamide is a solvatochromic fluorophore which exhibits large Stokes shifts in polar solvent,²⁹ while ^{DNS}C does not exhibit significant Stokes shift according to solvent change. Thus, we expected that the properties of dansyl were significantly changed by direct conjugation with cytosine. Next, we needed to investigate the properties of ^{DNS}C under a variety of pH conditions since cytosine is a pH sensitive molecule and can be protonated at low pH in order to form a biologically important structure, i-motif. As a result, we observed that the fluorescence of ^{DNS}C exhibited a high pH-dependency, with the inflection point at pH 6.9 (Fig. 3). Through NMR spectroscopic titration experiments (see Fig. S2 in ESI†),³⁰ we found that the protonation or deprotonation of ^{DNS}C underwent a transition at pH 6.8, consistent with the fluorescence data. We speculated that the pH-dependent fluorescence change resulted from deprotonation of ^{DNS}C that occurred at sulfonamide, the N4 position of the cytosine unit. Previous reports confirmed the decrease of the pK_a value of dansylamide (from 10.6 to 6.3) in the presence of the carbonyl group, which can stabilize the anionic form of dansylamide.³¹ Likewise, dansylamide in ^{DNS}C seemed to have a low pK_a value of 6.8 because of the stabilizing effect of the cytosine ring. We also observed a fluorescence enhancement on deprotonation of sulfonamide.^{31a,32} Accordingly, we concluded that the degree of deprotonation influences the fluorescence of ^{DNS}C .

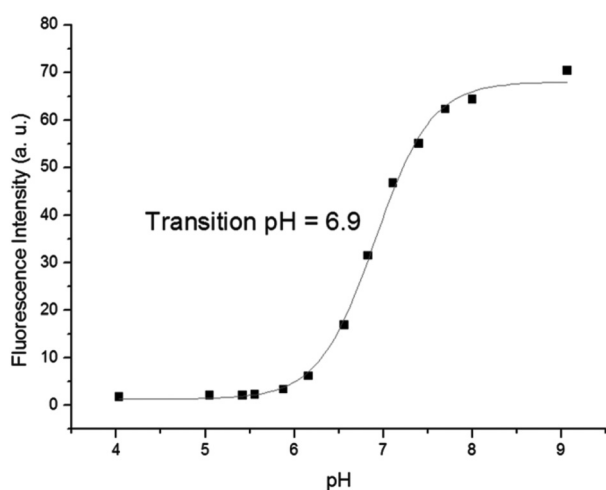


Fig. 3 Fluorescence intensity of ^{DNS}C plotted with respect to pH (concentration, 3 μ M; total volume, 1 mL; excitation, 295 nm).

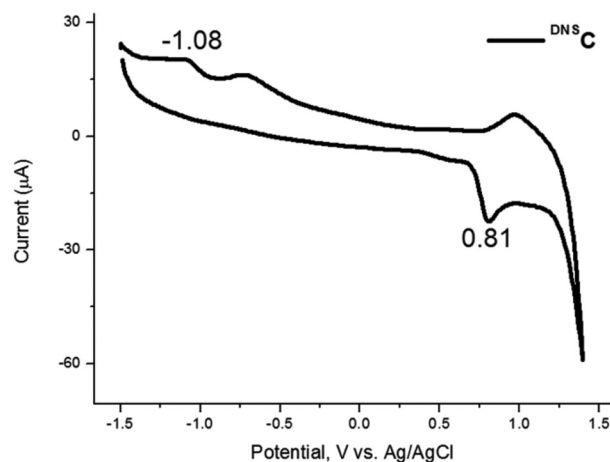


Fig. 4 Cyclic voltammogram of ^{DNS}C (3.4 mM aqueous solution containing 50% MeOH; supporting electrolyte, 100 mM KCl; reference electrode, Ag/AgCl; scan rate, 50 $mV s^{-1}$).

Similar solvent and pH-dependent fluorescence behavior has been observed previously for various other fluorescent nucleosides. For example, the fluorescence of 5-(1-pyrenyl)-modified pyrimidine exhibits significant pH-dependence.^{33–35} In particular, Py-dC displays very low fluorescence over the entire pH range, much like ^{DNS}C .^{12,33,35–37} Because the fluorescence of Py-dC can be quenched through proton-coupled electron transfer, we suspected that the luminescence of ^{DNS}C could also be quenched through a similar mechanism. To obtain evidence for this hypothesis, we measured the electrochemical potential of ^{DNS}C (Fig. 4), observing the oxidation potential of the dansyl group at +0.81 V and the reduction potential of the cytosine unit at -1.08 V, using a Ag/AgCl electrode. Accordingly, the dansyl moiety exhibited almost the same oxidation potential as that determined previously (+0.9 V),^{28a,38} whereas the reduction potential of the dansyl-modified cytosine unit was slightly lower than that of natural cytosine.³⁹ According to the Rehm–Weller equation,⁴⁰ $\Delta E(0,0)$ was equal to 2.96 eV (Fig. S4 in ESI†); together with the redox potential of ^{DNS}C , we determined the value of ΔG_{eT} to be -1.07 eV (-103 $kJ mol^{-1}$), implying that electron transfer would be energetically favored.

Study of the fluorescence behavior of ^{DNS}C in oligonucleotides

Next, we introduced ^{DNS}C into four types of 15-mer oligonucleotide (ODN) sequences containing different flanking bases. In previous studies, dansyl moieties have been conjugated to nucleosides in a variety of positions, including the C5 and C8 positions of the nucleobases and 2'-O position of the sugar ring.^{20–22} The same dansyl moiety can readily modify the fluorescence properties of ODNs merely by changing the position and linker for conjugation. We suspected that ODNs containing a ^{DNS}C residue might exhibit significant changes in fluorescence upon duplex formation, as a result of changes in the protonation state of its cytosine unit; in addition, we expected different neighboring bases to provide different environments

Table 3 ODN sequences investigated in this study

ODN	Sequence (5' to 3')
DNS-N ^a	GCT CTT N ^{DNS} CN TTC TCG
Nat-N ^a	GCT CTT NCN TTC TCG
ODN-X-Y ^b	CGA GAA YXY AAG AGC
DNS-Probe	A CCC TAA C ^{DNS} CC TAA C ^{DNS} CC TAA CCC T
Htelo	A(GGGTTA) ₃ GGGT

^a N = A, T, C, G. ^b X, Y = A, T, C, G.

for the ^{DNS}C residue in the ODNs, further influencing the fluorescence behavior.

We synthesized twenty-four 15-mer ODNs, including four modified sequences, and confirmed their masses using MALDI-TOF mass spectrometry (see Table 3 and Table S1 in ESI†). The four DNS-N strands (N = A, T, C, G) had the ^{DNS}C residue in the middle of the ODN with different flanking bases. We checked the basic UV absorptions and fluorescence emissions of the single- and double-strand forms of the DNS-N ODNs. Each DNS-N had 17 different states—including the single strand and fully matched and singly and triply mismatched double strands—when combined with the Nat-N sequences. We recorded all of these UV absorption and fluorescence emission spectra in a buffer solution at pH 9 in the absence of any salt.

First, we checked the CD spectra of all the strands mixed with DNS-C to confirm duplex formation. We observed positive and negative CD signatures for duplexes at 275 and 250 nm, respectively, even for those containing single or triple mismatches; in contrast, the single-stranded DNS-C exhibited very weak CD signals at these wavelengths (see Fig. S5 in ESI†). In the UV absorption spectra of these ODNs, we observed the same patterns, with an intense absorption at 260 nm, resulting from the absorptions of the natural nucleobases (see Fig. S6 in ESI†). Because ^{DNS}C absorbs at wavelengths of 295 and 330 nm, its absorption bands overlapped with those of the other residues in the ODNs. We could not detect any specific differences in the UV spectroscopic behavior of these ODNs; we did, however, observe unique phenomena in their fluorescence spectra. For DNS-C, we observed a three-fold enhancement in fluorescence only for its duplex with ODN-G-G, which contains a GGG triad in the middle of its sequence (Fig. 5). For a comparison of the fluorescence intensity, we estimated the fluorescence quantum yield of oligonucleotides by using the extinction coefficient. We assumed that ^{DNS}C have the same extinction coefficient even in oligonucleotides and calculated the absorbance from the concentration of oligonucleotides. We finally obtained 0.020 for duplex having GGG triad and 0.0056–0.0092 for the others. Compared to the nucleoside in aqueous solution, ^{DNS}C in oligonucleotides have similar quantum yields, which means that it was exposed to water. None of the duplexes containing mismatched sequences exhibited any enhancement of fluorescence. Notably, DNS-A, -T, and -G exhibited no fluorescence enhancements even in duplexes with their fully matched sequences in the absence of a salt (see Fig. 6 and Fig. S7 in ESI†). These findings confirmed

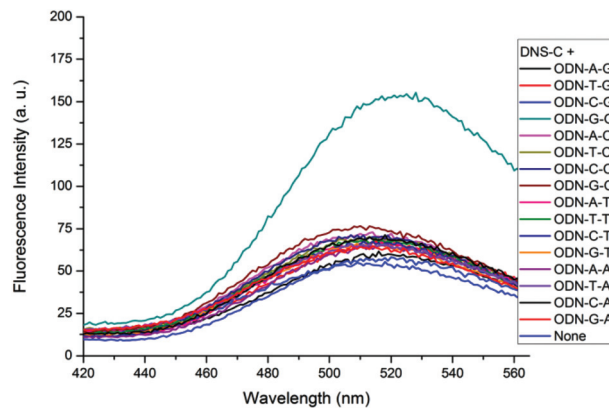


Fig. 5 Fluorescence emission spectra of DNS-C in duplexes with different triad sequences (concentration, 1.5 μ M; total volume, 1 mL; buffer, 100 mM Tris, pH 9.0; excitation, 295 nm, excitation and emission slit: 10 nm).

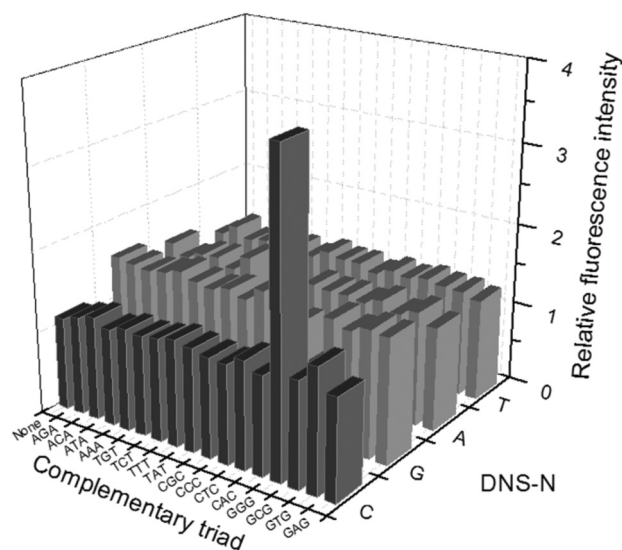


Fig. 6 Relative fluorescence emission intensities of DNS-N strands in the presence of various complementary triad sequences.

that the fluorescence of the ^{DNS}C residue is dependent on the nature of its complementary and flanking bases.

The unique fluorescence enhancement of the ^{DNS}C residue appears to be closely related to the stability of its duplex. In the presence of a salt, we observed a slightly increased fluorescence for all of the fully matched duplexes of DNS-A, -T, and -G (see Fig. S8 in ESI†). These results meant that the formation of a stable duplex might facilitate deprotonation of N4 position. Actually, according to previous studies, proton transfer from cytosine to guanine can occur in the G/C pair.⁴¹ Thus, we expected that this process may be favoured in the GGG triad because of the neighbouring strong G/C pair holding the ^{DNS}C/G pair together and the low pK_a value of ^{DNS}C leading to easy deprotection and fluorescence enhancement. From measurements of melting temperatures (*T*_m), we also observed the highest thermal stability for the duplex of DNS-C and ODN-G-G in the presence of salts (Table 4).

Table 4 Values of T_m of fully matched and single-base-mismatched duplexes of DNS-N strands

T_m (°C)	-C ^{DNS} CC- (DNS-C)	-G ^{DNS} CG- (DNS-G)	-A ^{DNS} CA- (DNS-A)	-T ^{DNS} CT- (DNS-T)
-NAN-	21.0 ^a (41.0) ^b	26.0 (43.4)	19.0 (36.7)	21.0 (40.1)
ΔT_m ^c	-3.0 (-4.0)	-1.0 (-3.6)	1.0 (-1.3)	6.0 (1.5)
-NTN-	17.2 (39.2)	20.2 (42.2)	17.7 (37.6)	13.1 (34.1)
ΔT_m	-7.0 (-6.0)	-5.0 (-3.0)	-1.5 (-2.6)	-5.0 (-6.1)
-NCN-	15.4 (36.4)	23.4 (44.3)	20.3 (39.3)	13.3 (34.4)
ΔT_m	-4.0 (-5.0)	1.0 (-0.1)	5.0 (3.0)	-1.0 (-3.0)
-NGN-	23.1 (44.6)	22.5 (42.5)	17.4 (39.5)	13.6 (35.6)
ΔT_m	-16.5 (-14.0)	-20.1 (-18.0)	-18.0 (-14.0)	-19.4 (-18.9)

^a Sample concentration, 1.5 μ M; buffer, 100 mM Tris (pH 9.0); without salt. ^b Sample concentration, 1.5 μ M; buffer, 100 mM Tris (pH 9.0), 100 mM NaCl, 20 mM MgCl₂. ^c Thermal stability differences with natural sequences (T_m of modified duplex - T_m of natural duplex).

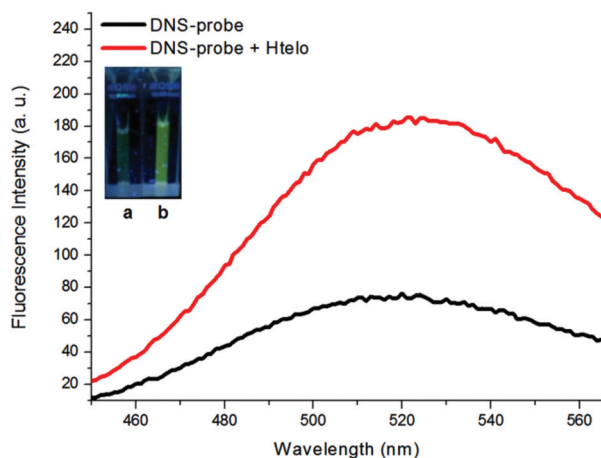


Fig. 7 Fluorescence enhancement upon duplex formation between DNS-Probe and Htelo. Inset: photograph of the fluorescence of (a) DNS-Probe and (b) DNS-Probe + Htelo (sample concentration, 1.5 μ M; total volume, 1 mL; buffer, 100 mM Tris, pH 9.0; excitation, 295 nm, excitation and emission slit: 10 nm).

Direct detection of the GGG triad sequence by ^{DNS}C

Based on previous results, we suggest that the fluorescence enhancement of a duplex is sensitive to its stability and to the nature of the bases neighboring the ^{DNS}C moiety; further studies will be necessary, however, to confirm the utility of ^{DNS}C for detection of GGG sequences. For that, we designed a simple fluorescent probe, DNS-Probe, for sensing the GGG triad position in complementary Htelo, a human G-quadruplex-forming sequence. As expected, DNS-Probe exhibited a three-fold enhancement of fluorescence in its duplex form (Fig. 7) and we could observe a fluorescence enhancement of DNS-Probe with the naked eye in the presence of Htelo. Accordingly, ^{DNS}C appears to be useful for the detection of biologically relevant sequences containing the GGG triad.

Study of the thermal stability of duplex containing ^{DNS}C

Furthermore, we checked the duplex stabilities of the DNS-N and Nat-N strands from their melting temperature curves recorded in the absence and presence of a salt. We expected that the DNS-N strands would exhibit novel types of interactions

with their complementary sequences because the electron-withdrawing sulfonyl group and aromatic ring of the dansyl moiety of the ^{DNS}C residue would modify the strength of the hydrogen bond between the cytosine and guanine bases. Indeed, ^{DNS}C exhibited different properties that differentiated it from natural deoxycytidine—primarily through disruption of the original hydrogen bonding pattern with guanine. We observed a highly destabilizing effect of the ^{DNS}C residue for the fully matched duplexes of the DNS-N strands in the presence of a salt (Table 4; $\Delta T_m = -14.0, -18.0, -14.0, -18.9$ °C, relative to the Nat-N strands). This destabilizing effect of ^{DNS}C was still maintained in single-mismatched duplexes. According to previous reports, exocyclic amine⁴² and exocyclic adduct⁴³ were deleterious to duplex stability due to steric hindrance of the bulky exocyclic group and the weakened hydrogen bond. Similarly, we suspected that steric hindrance existed between the dansyl unit and the flanking bases as a result of the almost perpendicular arrangement (the angle of N(2)-S(1)-C(12) is 106.72°, see Table S4 in ESI†) of the cytosine and dansyl moieties. As a result of this effect, the thermal stabilities of the fully matched and single-base-mismatched duplexes were similar, allowing ^{DNS}C to be used as a universal base. On the other hand, the destabilizing effect of ^{DNS}C was diminished in single-adenine-mismatched duplex (-NAN-) of DNS-C and -T (Table 4). For DNS-T, in particular, the single-adenine-mismatched duplex had a higher stability than the natural duplex ($\Delta T_m = +1.5$ °C) while the other single mismatched duplex exhibited a lower stability than the natural one ($\Delta T_m = -6.1, -3.0, -18.9$ °C, respectively). There should be interactions between adenine and ^{DNS}C bases, inducing a new type of weak ^{DNS}C/dA pair. To sum up, the dansyl group of ^{DNS}C seemed to distort the stable original G/C pair and to destabilize the entire duplex. However, ^{DNS}C exhibits the properties of a universal base, featuring even stability for all fully matched and single-base-matched duplexes. We also confirmed the unique stability of single-adenine-mismatched duplexes, although the stability of these duplexes was susceptible to the nature of the flanking bases.

Conclusions

The development of novel fluorescent nucleosides remains a challenging task for the sensitive detection of specific DNA

sequences and for monitoring the interactions between DNA strands and other biomolecules. The dansyl group is used widely as a fluorophore for nucleosides because it is sensitive to hydrophobic/hydrophilic conditions. Nevertheless, the quest remains for new dansyl-conjugated nucleosides that can provide more sensitive fluorescence detection of DNA systems. For that reason, we synthesized ^{DNS}C and characterized its photophysical properties. Relative to general dansyl-amides, ^{DNS}C exhibits more significant enhancements in fluorescence in response to changes in the polarity of the solvent, presumably resulting from PET from the dansyl group to the cytosine unit. Finally, we incorporated ^{DNS}C also into a series of 15-mer ODNs. Most dramatically, the DNS-C sequence exhibited a threefold enhancement in fluorescence after forming a duplex with a sequence containing a GGG triad sequence.

Clearly, ^{DNS}C exhibits properties quite different from those of the natural cytosine and dansyl group. Accordingly, we expect that the unique properties of fluorescent ^{DNS}C could be applied in several fluorescent systems for studying GGG triads, G-quadruplex or i-motif sequences, and DNA-protein interactions in due course.

Experimental

General experimental details

Each reaction was performed under anhydrous conditions under Ar or N₂. All reagents were purchased from Sigma-Aldrich, Fluka, Proligo, and Glen Research and were used without additional purification. Most solvents were used without distillation, except for those for phosphoramidite synthesis. High-resolution fast atom bombardment (HRMS-FAB) mass spectra were recorded using a Jeol JMS700 HR mass spectrometer at the Korea Basic Science Center, Daegu, Korea. MALDI-TOF mass spectra were recorded at Bioneer, Taejeon, Korea. ¹H NMR spectra were recorded using a FT-300 MHz Bruker Aspect 3000 spectrometer. UV and fluorescence spectra and *T_m* of oligonucleotides were recorded using Cary 100 and Eclipse spectrometers (Varian). Samples for UV/fluorescence spectroscopy were prepared in a quartz cell (path length: 1 cm). DNA synthesis was performed using a Polygen 12 synthesizer. An Agilent high-performance liquid chromatography system (1100 Series) was used to purify the synthesized ODNs; Agilent, ZORBA X Eclipse XDB-C18, 9.4 × 250 mm; gradient elution: 0 min, A:B = 90:10; 10 min, A:B = 90:10; 20 min, A:B = 0:100; 25 min, A:B = 0:100; 30 min, A:B = 90:10; solution A, 0.1 M triethylammonium acetate (TEAA) buffer (pH 7.2)-MeCN, 95:5; solution B, 0.1 M TEAA buffer (pH 7.2)-MeCN, 1:1; flow rate: 2.5 mL min⁻¹; UV detection: 254 nm.

Synthesis of 5'-O,3'-O-di-*tert*-butyldimethylsilyl-2'-deoxycytidine (1)

TBDMS-Cl (602 mg, 4.0 equiv.) was added to a solution of 2'-deoxycytidine (450 mg, 2 mmol) and imidazole (817 mg, 6.0

equiv.) in dry DMF and then the mixture was stirred at room temperature for 10 h. After concentrating, the residue was partitioned between CH₂Cl₂ (100 mL) and water (100 mL). The organic phase was washed with saturated NaCl (2 × 100 mL), dried (Na₂SO₄), and filtered. The solvent was evaporated and the residue was dried under reduced pressure. The crude product was purified through flash chromatography (SiO₂, EtOAc) to give a white solid **1** (800 mg, 88%). TLC: *R_f* = 0.18 (EtOAc); m.p. = 178–180 °C; ¹H NMR (300 MHz, DMSO-d₆, 25 °C): δ = 0.07 (12H, s, SiCH₃), 0.87 (9H, s, *t*-Bu), 0.88 (9H, s, *t*-Bu), 1.97–2.06 (1H, m, 2'-H), 2.10–2.18 (1H, m, 2'-H), 3.67–3.81 (3H, m, 5'-H, 3'-H), 4.32–4.36 (1H, m, 4'-H), 5.70 (1H, d, *J* = 7.5 Hz, 5-H), 6.15 (1H, t, *J* = 6.3 Hz, 1'-H), 7.16 (2H, br, N4-H), 7.70 (1H, d, *J* = 7.2 Hz, 6-H); ¹³C NMR (75 MHz; DMSO-d₆, 25 °C): δ = -5.7, -5.6, -5.0, -4.8, 17.6, 17.9, 25.6, 25.7, 62.3, 71.4, 84.5, 86.4, 93.8, 140.3, 154.9, 165.5; HRMS-FAB MS (*m/z*): calcd for C₂₁H₄₁N₃O₄Si₂ [M + Na]⁺: 478.2534; found: 478.2536.

Synthesis of 4-*N*-dansyl-5'-O, 3'-O-di-*tert*-butyldimethylsilyl-2'-deoxycytidine (2)

Compound **1** (517 mg, 1.13 mmol) and dansyl chloride (457 mg, 1.5 equiv.) were dried under vacuum for 2 h and then they were dissolved in dry CH₂Cl₂ (20 mL) and stirred under Ar. DIPEA (0.3 mL, 2.0 equiv.) was added and then the mixture was stirred for 24 h. The solvent was evaporated under vacuum and the residue was partitioned between CH₂Cl₂ (100 mL) and water (100 mL). The organic phase was washed with saturated NaCl (2 × 100 mL), dried (Na₂SO₄), and filtered. The product was purified through column chromatography (SiO₂, CH₂Cl₂ to CH₂Cl₂-EtOAc = 1:1) to yield a pale-yellow product **2** (546 mg, 70%). TLC: *R_f* = 0.88 (CH₂Cl₂-EtOAc = 4:1); m.p. = 103–105 °C; ¹H NMR (300 MHz, DMSO-d₆, 25 °C): δ = 0.03 (12H, s, SiCH₃), 0.83 (18H, s, SiCH₃), 2.11–2.29 (2H, m, 2'-H), 2.81 (6H, s, N-CH₃), 3.65–3.80 (3H, m, 5'-H, 3'-H), 4.30–4.31 (1H, m, 4'-H), 5.96 (1H, t, *J* = 5.4 Hz, 1'-H), 6.38 (1H, d, *J* = 8.1 Hz, 5-H), 7.23 (1H, d, *J* = 7.2 Hz, PhH), 7.56 (1H, t, *J* = 8.7 Hz, PhH), 7.62 (1H, t, *J* = 7.5 Hz, PhH), 7.89 (1H, d, *J* = 8.1 Hz, 6-H), 8.20 (1H, d, *J* = 8.4 Hz, PhH), 8.32 (1H, d, *J* = 8.7 Hz, PhH), 8.43 (1H, d, *J* = 8.4 Hz, PhH), 12.22 (1H, s, N4-H); ¹³C NMR (75 MHz; DMSO-d₆, 25 °C): δ = -5.7, -5.1, -4.8, 17.6, 17.9, 25.6, 45.0, 61.7, 70.3, 85.2, 86.8, 95.4, 115.0, 120.2, 123.5, 126.8, 127.5, 129.0, 129.1, 129.3, 138.3, 142.3, 148.3, 151.1, 159.8; HRMS-FAB MS (*m/z*): calcd for C₃₃H₅₂N₄O₆SSi [M⁺]: 688.3146; found: 688.3149.

Synthesis of 4-*N*-dansyl-2'-deoxycytidine (^{DNS}C)

THF (10 mL) and 1 M tetrabutylammonium fluoride (TBAF, 2.1 mL, 4 equiv.) were added to compound **2** (360 mg, 0.52 mmol) and then the mixture was stirred at room temperature for 6 h. The solvent was evaporated and then CH₂Cl₂ was added to the residue, which was purified through column chromatography (SiO₂; CH₂Cl₂-MeOH, from 20:1 to 10:1) to obtain a yellow compound ^{DNS}C (233 mg, 97%). TLC: *R_f* = 0.41 (CH₂Cl₂-MeOH = 9:1); m.p. = 128–130 °C; ¹H NMR (300 MHz, DMSO-d₆, 25 °C): δ = 2.05–2.11 (2H, m, 2'-H), 2.80 (6H, s,

NCH₃), 3.50–3.55 (2H, m, 5'-H), 3.75–3.78 (1H, m, 3'-H), 4.15–4.18 (1H, m, 4'-H), 5.00 (1H, t, $J = 5.4$ Hz, 5'-OH), 5.23 (1H, d, $J = 4.5$ Hz, 3'-OH), 6.02 (1H, t, $J = 6.3$ Hz, 1'-H), 6.39 (1H, d, $J = 8.1$ Hz, 5-H), 7.22 (1H, d, $J = 7.5$ Hz, PhH), 7.56 (1H, t, $J = 8.4$ Hz, PhH), 7.63 (1H, t, $J = 8.1$ Hz, PhH), 8.03 (1H, d, $J = 7.8$ Hz, 6-H), 8.24 (1H, d, $J = 7.2$ Hz, PhH), 8.34 (1H, d, $J = 8.7$ Hz, PhH), 8.43 (1H, d, $J = 8.4$ Hz, PhH), 12.19 (1H, br, N4-H); ¹³C NMR (75 MHz; DMSO-d₆, 25 °C): $\delta = 45.1, 48.6, 61.0, 70.0, 85.3, 87.8, 95.9, 115.1, 120.3, 123.6, 126.9, 127.6, 129.1, 129.2, 129.4, 138.3, 142.8, 148.6, 151.2, 160.0$; HRMS-FAB MS (m/z): calcd for C₂₁H₂₄N₄O₆S [M⁺]: 460.1417; found: 460.1420.

Synthesis of 4-*N*-dansyl-5'-*O*-dimethoxytrityl-2'-deoxycytidine (3)

DIPEA (0.89 mL, 10 equiv.) was added to a solution of ^{DNS}C (233 mg, 0.51 mmol) in dry DMF. After 1 h, DMT-Cl (260 mg, 1.5 equiv.) was added and then the mixture was stirred at 55–60 °C for 10 h. After quenching the reaction with MeOH (2 mL), the mixture was stirred for 1 h. After concentrating, the residue was partitioned between CH₂Cl₂ (100 mL) and NaHCO₃ (100 mL). The organic layer was washed with saturated NaCl (2 × 100 mL), dried (Na₂SO₄), and filtered. The solvent was evaporated and the residue was dried under reduced pressure. The crude product was purified through flash chromatography (SiO₂; hexane–EtOAc, from 3 : 1 to 1 : 1) to give a yellow solid 3 (311 mg, 80%). TLC: $R_f = 0.21$ (hexane–EtOAc = 1 : 1); m.p. = 132–134 °C; ¹H NMR (300 MHz, DMSO-d₆, 25 °C): $\delta = 2.05$ –2.14 (2H, m, 2'-H), 2.80 (6H, s, NCH₃), 3.25–3.30 (2H, m, 5'-H), 3.75 (6H, s, OCH₃), 3.85–3.87 (1H, m, 3'-H), 4.27–4.30 (1H, m, 4'-H), 5.31 (1H, m, 3'-OH), 6.00 (1H, t, $J = 5.4$ Hz, 1'-H), 6.23 (1H, d, $J = 7.8$ Hz, 5-H), 6.89 (4H, d, $J = 6.6$ Hz, PhH), 7.22–7.37 (10H, m, PhH), 7.52–7.58 (2H, m, PhH), 7.89 (1H, d, $J = 8.1$ Hz, 6-H), 8.11 (1H, d, $J = 6.9$ Hz, PhH), 8.32 (1H, d, $J = 8.4$ Hz, PhH), 8.42 (1H, d, $J = 8.4$ Hz, PhH), 12.21 (1H, br, N4-H); ¹³C NMR (75 MHz; DMSO-d₆, 25 °C): $\delta = 45.0, 55.0, 62.6, 69.0, 85.0, 85.5, 85.9, 95.7, 113.2, 115.0, 120.2, 123.4, 126.8, 127.5, 127.7, 127.9, 129.3, 129.6, 129.8, 135.1, 135.5, 138.2, 142.5, 144.5, 148.3, 151.2, 158.1, 159.8$; HRMS-FAB MS (m/z): calcd for C₄₂H₄₄N₄O₈S [M⁺]: 762.2723; found: 762.2720.

Crystal data for ^{DNS}C (C₂₁H₂₄N₄O₆S)

A crystal of ^{DNS}C was coated with paratone-N oil and its diffraction data measured at 95 K with synchrotron radiation ($\lambda = 0.72999$ Å) on an ADSC Quantum-210 detector at 2D SMC with a Si (111) double crystal monochromator (DCM) at the Pohang Accelerator Laboratory, Korea. The ADSC Q210 ADX program⁴⁴ was used for data collection and HKL3000sm (v. 703r) software⁴⁵ was used for cell refinement, reduction, and absorption correction. The crystal structure of ^{DNS}C was solved using the direct method and refined through full-matrix least-squares calculations with the SHELXL-TL (v. 2008) program package.⁴⁶ All non-hydrogen atoms were refined anisotropically. The hydrogen atoms were assigned isotropic displacement coefficients [$U(H) = 1.2U(C,N)$ or $1.5U(C_{\text{methyl}})$] and their

coordinates were allowed to ride on their respective atoms. None of the hydrogen atoms on carbon atoms were included during the least-squares refinement. Refinement of the structure converged at a final value of R_1 of 0.0385 and R_2 of 0.1072 for 4600 reflections [with $I > 2\sigma(I)$] ($R_1 = 0.0434$ and $wR_2 = 0.1019$ for all reflections). The largest difference peak and hole were 0.886 and -0.439 e Å⁻³, respectively. A summary of the crystallographic data and refinement parameters is given in the ESI (Table S2–S6, and Fig. S9 in ESI†). CCDC 930728 contains the supplementary crystallographic data for this paper.

Computational details

All quantum chemical calculations were performed with a developmental version of Q-Chem.²³ Geometry optimization of ^{DNS}C was undertaken at the B3LYP/6-31G(d) level.²⁴ The obtained geometry was utilized for calculations of excited state energies. The SOS-CIS(D₀) method with the 6-31G(d) basis set was adopted for computing the excited state properties because this method provides a reliable behavior for charge-transfer excited states and quasi-degenerate excited states.²⁵ The solvent effect was considered by adopting COSMO.²⁶

Cyclic voltammetry

A solution of ^{DNS}C (3.4 mM) was prepared in 50% aqueous MeOH. The electrolyte was 100 mM KCl. The redox potential of ^{DNS}C was measured using a Model 263A potentiostat/galvanostat (Princeton Applied Research) at a scan rate of 100 mV s⁻¹ and over a scan range of ± 1.5 V. Two carbon electrodes were employed as the working and counter electrodes; a saturated Ag/AgCl electrode was used as the reference electrode.

Acknowledgements

We thank the EPB Center Program of MEST/NRF (20120000528) and the NRF of Korea (2012R1A2A2A01047069) for financial support and H. C. Jeon for help with the cyclic voltammetry experiments.

Notes and references

- 1 D. M. Kolpashchikov, *Chem. Rev.*, 2010, **110**, 4709–4723.
- 2 N. Venkatesan, Y. J. Seo and B. H. Kim, *Chem. Soc. Rev.*, 2008, **37**, 648–663.
- 3 A. Okamoto, *Chem. Soc. Rev.*, 2011, **40**, 5815–5828.
- 4 H. Zhang, F. Li, B. Dever, X.-F. Li and X. C. Le, *Chem. Rev.*, 2013, **113**, 2812–2841.
- 5 N. Dai and E. T. Kool, *Chem. Soc. Rev.*, 2011, **40**, 5756–5770.
- 6 J. Liu, Z. Cao and Y. Lu, *Chem. Rev.*, 2009, **109**, 1948–1998.
- 7 S. Sasaki, K. Onizuka and Y. Taniguchi, *Chem. Soc. Rev.*, 2011, **40**, 5698–5706.

- 8 (a) Y. J. Seo, I. J. Lee, J. W. Yi and B. H. Kim, *Chem. Commun.*, 2007, 2817–2819; (b) Y. J. Seo and B. H. Kim, *Chem. Commun.*, 2006, 150–152; (c) Y. J. Seo, I. J. Lee and B. H. Kim, *Bioorg. Med. Chem. Lett.*, 2008, **18**, 3910–3912; (d) I. J. Lee, J. W. Yi and B. H. Kim, *Chem. Commun.*, 2009, 5383–5385; (e) I. J. Lee and B. H. Kim, *Chem. Commun.*, 2012, **48**, 2074–2076.
- 9 Y. N. Teo and E. T. Kool, *Chem. Rev.*, 2012, **112**, 4221–4245.
- 10 D. Dziuba, V. Y. Postupalenko, M. Spadafora, A. S. Klymchenko, V. Guérineau, Y. Mély, R. Benhida and A. Burger, *J. Am. Chem. Soc.*, 2012, **134**, 10209–10213.
- 11 R. W. Sinkeldam, N. J. Greco and Y. Tor, *Chem. Rev.*, 2010, **110**, 2579–2619.
- 12 H.-A. Wagenknecht, *Nat. Prod. Rep.*, 2006, **23**, 973–1006.
- 13 (a) G. T. Hwang, Y. J. Seo and B. H. Kim, *J. Am. Chem. Soc.*, 2004, **126**, 6528–6529; (b) J. H. Ryu, Y. J. Seo, G. T. Hwang, J. Y. Lee and B. H. Kim, *Tetrahedron*, 2007, **63**, 3538–3547.
- 14 W. E. Wright, V. M. Tesmer, K. E. Huffman, S. D. Levene and J. W. Shay, *Genes Dev.*, 1997, 2801–2809.
- 15 T. A. Brooks, S. Kendrick and L. Hurley, *FEBS J.*, 2010, **277**, 3459–3469.
- 16 M. Gardiner-Garden and M. Frommer, *J. Mol. Biol.*, 1987, **196**, 261–282.
- 17 (a) D. M. Chenoweth, J. A. Poposki, M. A. Marques and P. B. Dervan, *Bioorg. Med. Chem.*, 2007, **15**, 759–770; (b) C. Tisné, B. Hartmann and M. Delepierre, *Biochemistry*, 1999, **38**, 3883–3894.
- 18 (a) F. D. Jones and S. H. Hughes, *Virology*, 2007, **360**, 341–349; (b) J. G. Julias, M. J. McWilliams, S. G. Sarafianos, W. G. Alvord, E. Arnold and S. H. Hughes, *J. Virol.*, 2004, **78**, 13315–13324.
- 19 J. R. Lakowicz, *Principles of Fluorescence Spectroscopy*, Springer, New York, 3rd edn, 2006, ch. 3, pp. 67–68.
- 20 A. Misra, S. Mishra and K. Misra, *Bioconjugate Chem.*, 2004, **15**, 638–646.
- 21 D. A. Barawkar and K. N. Ganesh, *Nucleic Acids Res.*, 1995, **23**, 159–164.
- 22 D. Singh, V. Kumar and K. N. Ganesh, *Nucleic Acids Res.*, 1990, **18**, 3339–3345.
- 23 Y. Shao, L. Fusti-Molnar, Y. Jung, J. Kussmann, C. Ochsenfeld, S. T. Brown, A. T. B. Gilbert, L. V. Slipchenko, S. V. Levchenko, D. P. O'Neill, R. A. Distasio Jr., R. C. Lochan, T. Wang, G. J. O. Beran, N. A. Besley, J. M. Herbert, C. Y. Lin, T. Van Voorhis, S. H. Chien, A. Sodt, R. P. Steele, V. A. Rassolov, P. E. Maslen, P. P. Korambath, R. D. Adamson, B. Austin, J. Baker, E. F. C. Byrd, H. Dachsel, R. J. Doerksen, A. Dreuw, B. D. Dunietz, A. D. Dutoi, T. R. Furlani, S. R. Gwaltney, A. Heyden, S. Hirata, C.-P. Hsu, G. Kedziora, R. Z. Khallulin, P. Klunzinger, A. M. Lee, M. S. Lee, W. Liang, I. Lotan, N. Nair, B. Peters, E. I. Proynov, P. A. Pieniazek, Y. M. Rhee, J. Ritchie, E. Rosta, C. D. Sherrill, A. C. Simmonett, J. E. Subotnik, H. L. Woodcock III, W. Zhang, A. T. Bell, A. K. Chakraborty, D. M. Chipman, F. J. Keil, A. Warshel, W. J. Hehre, H. F. Schaefer III, J. Kong, A. I. Krylov, P. M. W. Gill and M. Head-Gordon, *Phys. Chem. Chem. Phys.*, 2006, **8**, 3172–3191.
- 24 (a) A. D. Becke, *Phys. Rev. A*, 1988, **38**, 3098–3100; (b) C. Lee, W. Yang and R. G. Parr, *Phys. Rev. B: Condens. Matter*, 1988, **37**, 785–789.
- 25 (a) D. Casanova, Y. M. Rhee and M. Head-Gordon, *J. Chem. Phys.*, 2008, **128**, 164106; (b) Y. M. Rhee, D. Casanova and M. Head-Gordon, *J. Phys. Chem. A*, 2009, **113**, 10564–10576.
- 26 A. Klamt, V. Jonas, T. Bürger and J. C. W. Lohrenz, *J. Phys. Chem. A*, 1998, **102**, 5074–5085.
- 27 A. Sharonov, T. Gustavsson, V. Carré, E. Renault and D. Markovitsi, *Chem. Phys. Lett.*, 2003, **380**, 173–180.
- 28 (a) P. Ceroni, I. Laghi, M. Maestri, V. Balzani, S. Gestermann, M. Gorka and F. Vögtle, *New J. Chem.*, 2002, **26**, 66–75; (b) U. Subuddhi, P. K. Vuram, A. K. Mishra and A. Chadha, *J. Photochem. Photobiol., A Chem.*, 2011, **217**, 411–416.
- 29 K. A. Fletcher, I. A. Storey, A. E. Hendricks, S. Pandey and S. Pandey, *Green Chem.*, 2001, **3**, 210–215.
- 30 E. D. Becker, H. T. Miles and R. B. Bradley, *J. Am. Chem. Soc.*, 1965, **87**, 5575–5582.
- 31 (a) R. Métivier, I. Leray and B. Valeur, *Photochem. Photobiol. Sci.*, 2004, **3**, 374–380; (b) S. Aoki, H. Kawatani, T. Goto, E. Kimura and M. Shiro, *J. Am. Chem. Soc.*, 2001, **123**, 1123–1132.
- 32 T. Koike, T. Watanabe, S. Aoki, E. Kimura and M. Shiro, *J. Am. Chem. Soc.*, 1996, **118**, 12696–12703.
- 33 R. Huber, T. Fiebig and H.-A. Wagenknecht, *Chem. Commun.*, 2003, 1878–1879.
- 34 T. L. Netzel, M. Zhao, K. Nafisi, J. Headrick, M. S. Sigman and B. E. Eaton, *J. Am. Chem. Soc.*, 1995, **117**, 9119–9128.
- 35 N. Amann, E. Pandurski, T. Fiebig and H.-A. Wagenknecht, *Angew. Chem., Int. Ed.*, 2002, **41**, 2978–2980.
- 36 A. Kumar and M. D. Sevilla, *Chem. Rev.*, 2010, **110**, 7002–7023.
- 37 M. Raytchev, E. Mayer, N. Amann, H.-A. Wagenknecht and T. Fiebig, *ChemPhysChem*, 2004, **5**, 706–712.
- 38 J. Guy, K. Caron, S. Dufresne, S. W. Michnick, W. G. Skene and J. W. Keillor, *J. Am. Chem. Soc.*, 2007, **129**, 11969–11977.
- 39 S. Steenken, J. P. Telo, H. M. Novais and L. P. Candeias, *J. Am. Chem. Soc.*, 1992, **114**, 4701–4709.
- 40 J. R. Lakowicz, *Principles of Fluorescence Spectroscopy*, Springer, New York, 3rd edn, 2006, ch. 9, pp. 337–338.
- 41 (a) J. P. C. Carrasco, A. Requena and J. Zúñiga, *J. Phys. Chem. A*, 2009, **113**, 10549–10556; (b) S. Xiao, L. Wang, Y. Liu, X. Lin and H. Liang, *J. Chem. Phys.*, 2012, **137**, 195101; (c) Y. Lin, H. Wang, S. Gao and H. F. Schaefer III, *J. Phys. Chem. B*, 2011, **115**, 11746–11756.
- 42 (a) K. Kropachev, M. Kolbanovskiy, Z. Liu, Y. Cai, L. Zhang, A. G. Schwaib, A. Kolbanovskiy, S. Ding, S. Amin, S. Broyde and N. E. Geacintov, *Chem. Res. Toxicol.*, 2013, **26**, 783–793; (b) Y. Cai, N. E. Geacintov and S. Broyde, *Biochemistry*, 2012, **51**, 1486–1499; (c) F. A. Rodríguez, Y. Cai, C. Lin,

- Y. Tang, A. Kolbanovskiy, S. Amin, D. J. Patel, S. Broyde and N. E. Geacintov, *Nucleic Acids Res.*, 2007, **35**, 1555–1568.
- 43 C. A. Gelfand, G. E. Plum, A. P. Grollman, F. Johnson and K. J. Breslauer, *Biochemistry*, 1998, **37**, 12507–12512.
- 44 A. J. Arvai and C. Nielsen, *ADSC Quantum-210 ADX Program*, Area Detector System Corporation, Poway, CA, USA, 1983.
- 45 Z. Otwinowski and W. Minor, in *Methods in Enzymology*, ed. C. W. Carter Jr. and R. M. Sweet, Academic Press, New York, 1997, vol. 276, part A, p. 307.
- 46 G. M. Sheldrick, *SHELXTL-PLUS, Crystal Structure Analysis Package*, Bruker Analytical X-Ray, Madison, WI, USA, 1997.